JACS
JOURNAL OF THE AMERICAN CHEMICAL SOCIETY

Communication

pubs.acs.org/JACS

$Cu_2ZnGeSe_4$ Nanocrystals: Synthesis and Thermoelectric Properties

Maria Ibáñez,[†] Reza Zamani,[‡,§] Aaron LaLonde,[∥] Doris Cadavid,[‡] Wenhua Li,[‡] Alexey Shavel,[‡] Jordi Arbiol,[§,⊥] Joan Ramon Morante,[†,‡] Stéphane Gorsse,[#] G. Jeffrey Snyder,[∥] and Andreu Cabot*[,†,‡]

[†]Departament Electronica, Universitat de Barcelona, Barcelona 08028, Spain

[‡]Catalonia Energy Research Institute (IREC), Jardi de les Dones de Negre 1, Sant Adria del Besos, Barcelona 08930, Spain

[§]Institut de Ciència de Materials de Barcelona (ICMAB-CSIC), Campus de la UAB, Bellaterra 08193, Spain

[∥]Materials Science, California Institute of Technology, 1200 East California Boulevard, Pasadena, California 91125, United States

[⊥]Institució Catalana de Recerca i Estudis Avançats (ICREA), Barcelona 08010, Spain

[#]CNRS, Université de Bordeaux, ICMCB, 87 avenue du Docteur Albert Schweitzer, 33608 Pessac Cedex, France

Supporting Information

ABSTRACT: A synthetic route for producing $Cu_2ZnGeSe_4$ nanocrystals with narrow size distributions and controlled composition is presented. These nanocrystals were used to produce densely packed nanomaterials by hot-pressing. From the characterization of the thermoelectric properties of these nanomaterials, $Cu_2ZnGeSe_4$ is demonstrated to show excellent thermoelectric properties. A very preliminary adjustment of the nanocrystal composition has already resulted in a figure of merit of up to 0.55 at 450 °C.

The ample chemical and structural freedom of quaternary diamond-like chalcogenides allows their use in multiple applications, such as photovoltaics,[1,2] nonlinear optics,[3] thermoelectrics,[4,5] and even topological insulators, as recently demonstrated.[6,7] In particular, in the field of photovoltaics, copper-based quaternary diamond-like semiconductors of the family I_2−II−IV−VI_4 have recently gained a great deal of attention as alternatives to CdTe and $Cu(In,Ga)Se_2$ for use as absorber materials. The possibility of engineering quaternary semiconductors made of relatively low cost, abundant, and nontoxic elements having an optimum direct band gap has drawn high interest in the preparation and characterization of this class of materials, particularly $Cu_2ZnSn(S,Se)_4$.[1,2,8]

On the other hand, the complexity of the crystallographic structures of quaternary compounds is associated with intrinsically low thermal conductivities. In addition, the control of their composition allows for the tuning of their charge carrier concentration. Moreover, in the particular case of compositionally layered structures such as stannite, high electrical conductivities can coexist with large Seebeck coefficients and intrinsically low thermal conductivities. Thus, these quaternary compounds are also potentially excellent thermoelectric materials.[4,5,9]

While in photovoltaics the reduction of the lattice dimensions to the nanoscale allows for low-cost solution processing of devices, in the thermoelectrics field, nanostructuring further allows improvement of their efficiency.[10,11] Mainly, the reduction of the crystal domains to the nanoscale introduces a high density of phonon scattering centers, which reduce the material's thermal conductivity and enhance its thermoelectric figure of merit.

$Cu_2ZnGeSe_4$ (CZGS) is a p-type semiconductor with a direct band gap between 1.21 and 1.63 eV, as determined experimentally and theoretically.[12−15] Its ideal band gap makes it an alternative indium- and cadmium-free absorber material for photovoltaics.[15−18] CZGS crystallizes in a non-centered tetragonal structure with space group $I\bar{4}2m$.[19−21] Its quaternary nature, variety of ionic valences, and particular crystallographic structure suggest that CZGS should be characterized by intrinsically low thermal conductivities and potentially high electrical conductivities and Seebeck coefficients. This combination of properties qualifies CZGS as a potentially outstanding thermoelectric material.

In this communication, a synthetic route for producing CZGS nanoparticles with narrow size distributions and controlled composition is presented. This is the first presented synthetic route for the production of CZGS nanocrystals. Furthermore, the potential of CZGS as a thermoelectric material is demonstrated by characterizing the thermoelectric properties of CZGS nanocrystals with two different compositions.

CZGS nanoparticles were prepared by reacting metal complexes with an excess of selenium in octadecene. In a typical synthesis, 0.50 mmol of CuCl, 0.50 mmol of ZnO, 0.25 mmol of $GeCl_4$, 5 mM hexadecylamine, 0.1 mmol of *n*-tetradecylphosphonic acid, and 10 mL of octadecene were placed in a four-neck flask and heated to 200 °C under and argon flow. Separately, a 0.8 M selenium solution was prepared under argon by dissolving selenium dioxide in octadecene at 180 °C. A 4 mL aliquot of the precursor Se solution was injected into the heated solution containing the metal complexes at 295 °C. The solution was kept at this temperature for 5 min to allow the nanoparticles to grow. Finally, the flask was rapidly cooled to room temperature.

Figure 1 shows a representative transmission electron microscopy (TEM) micrograph of CZGSe nanoparticles produced by the procedure detailed here. Narrow size distributions, with dispersions below 10%, were systematically

Received: December 22, 2011
Published: February 14, 2012

   dx.doi.org/10.1021/ja211952z | *J. Am. Chem. Soc.* 2012, 134, 4060−4063

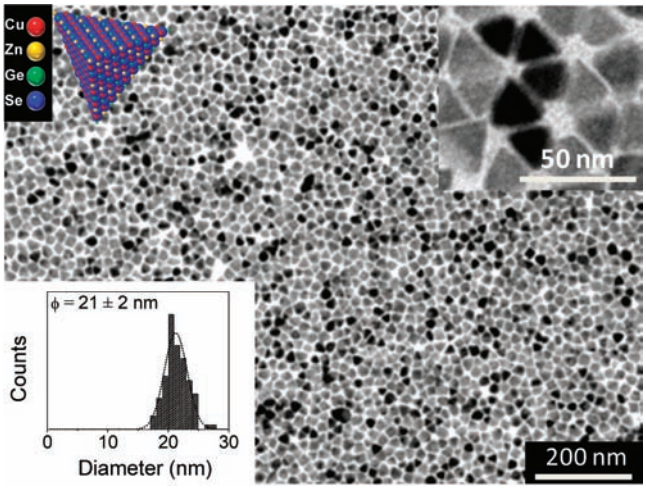

Figure 1. Representative TEM micrograph of the CZGS nanoparticles produced. The insets show an atomic model of the tetrahedral particle, a higher-magnification TEM micrograph, and the histogram with the measured particle size distribution.

obtained. The prepared nanocrystals typically showed tetragonal geometries (Figure 1 insets). The average nanoparticle size could be controlled by the reaction time and temperature in the range from 10 to 25 nm. Because of the particular kinetics of reaction of the different elements with selenium, we were unable to produce smaller nanocrystals with the stoichiometric composition.

As determined by energy dispersive X-ray spectroscopy (EDX) and confirmed by inductively coupled plasma spectrometry (ICP) analysis, the overall composition of the initially formed nanocrystals was very rich in Cu and Se and very poor in Zn and Ge. A few minutes of reaction time were necessary to obtain nanocrystals with the stoichiometric composition. Single-particle chemical analysis by electron energy loss spectroscopy (EELS) confirmed that the nanoparticles obtained after 10 s of reaction were mostly composed of Cu and Se (Figure 2A). It should be pointed out that the purification of these initial nanocrystals was not an easy task because of the large amount of unreacted complex in the solution. This explains the relatively large concentration of Zn and Ge detected by EELS outside the particles. After longer reaction time, single-particle analyses proved the presence of all four elements within each nanocrystal in the correct composition. It was further confirmed that the four elements were homogeneously distributed throughout the nanocrystal (Figure 2B). High-resolution TEM (HRTEM) analysis of the nanocrystals verified their tetragonal structure with lateral facets corresponding to {112} planes (Figure 2C).

The differences in the reaction kinetics of Cu, Zn, and Ge with Se allow for the adjustment of the nanoparticle composition inside a relatively wide range by control of the reaction time and temperature and by adjustment of the concentration of the different elements in the precursor solution. Figure 2E shows a ternary diagram with the composition distribution of two samples with different global compositions: $Cu_2ZnGeSe_4$ and $Cu_{2.15}Zn_{0.85}GeSe_{3.9}$. On the same graph, the average value of the single-particle analysis is

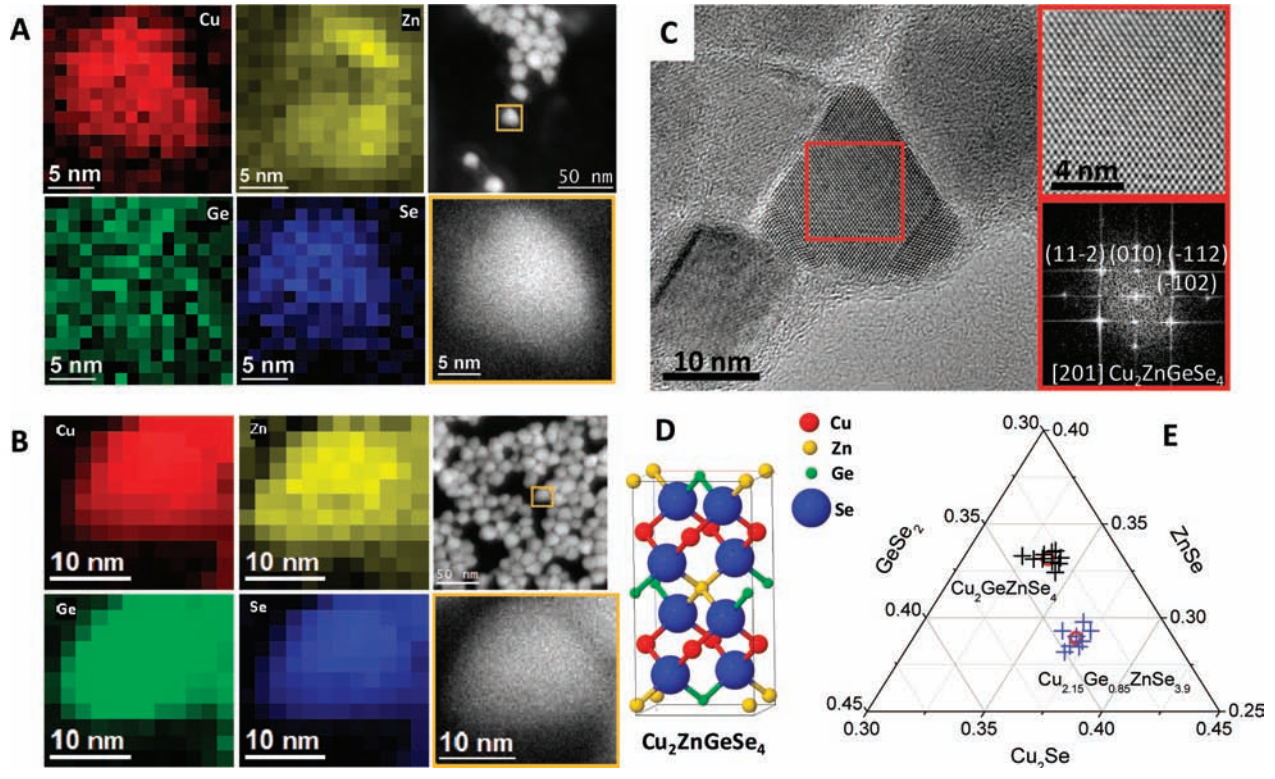

Figure 2. (A, B) HAADF images of a few nanoparticles and a single nanoparticle (right panels) and Cu, Zn, Ge and Se EELS compositional maps of the same single particle (left and center panels) obtained after reaction times of (A) 10 s and (B) 5 min. (C) HRTEM image and power spectrum analysis of a $Cu_2ZnGeSe_4$ nanoparticle. (D) Schematic illustration of the tetragonal structure of CZGS. (E) Ternary diagram showing the compositions of single nanoparticles obtained by HRTEM–EDX. The red circle shows the average value of the single-particle analysis, which is in good agreement with the results of the SEM–EDX, EELS, and ICP analyses.

dx.doi.org/10.1021/ja211952z | J. Am. Chem. Soc. 2012, 134, 4060–4063

also indicated. This is in good agreement with the results of the SEM–EDX, EELS, and ICP analyses performed.

Figure 3 shows the X-ray diffraction (XRD) patterns of the obtained nanocrystals, which resemble that of a tetragonal-

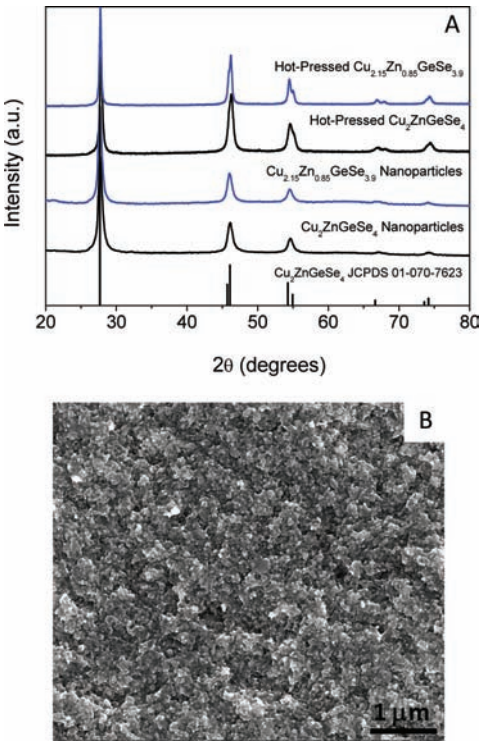

Figure 3. (A) XRD pattern of the $Cu_2ZnGeSe_4$ and $Cu_{2.15}Zn_{0.85}GeSe_{3.9}$ nanoparticles before and after hot-pressing. As a reference, the pattern corresponding to the tetragonal CZGS phase (space group $I\bar{4}2m$, JCPDS no. 01-070-7623) is also shown. (B) SEM image of the nanomaterial obtained after hot-pressing.

symmetry structure with the $I\bar{4}2m$ space group (JCPDS no. 01-070-7623).[20] No secondary phases were detected in either the stoichiometric sample or the copper-rich $Cu_{2.15}Zn_{0.85}GeSe_{3.9}$ sample.

The high yield of the previously detailed synthetic route allowed the procedure to be scaled up for the production of grams of nanocrystals with similarly narrow size distributions and controlled compositions. For thermoelectric characterization, roughly 2 g of nanoparticles of each of the two compositions tested were prepared. The nanocrystals were thoroughly washed by multiple precipitation and redispersion steps. The final nanoparticles could not be redispersed in organic solvents, proving the high degree of surfactant removal. Washed nanocrystals were dried of solution under an argon atmosphere. To remove completely the remaining residual organic ligands, the nanocrystals were heated to 500 °C for 1 h under an Ar flow inside a tube furnace. The annealed nanoparticles were ground into a fine powder. This nanopowder was hot-pressed under an Ar atmosphere at 40 MPa and 500 °C for 5 min. The density of the 12 mm pellets obtained was in the range 92–96%, as calculated from their weight and volume.

Figure 3B shows an SEM image of the material obtained after hot-pressing. The crystal domain size increased by a factor of ~1.7 upon annealing and hot-pressing treatment, as calculated from the fitting of the XRD patterns. In the particular case of the materials used for thermoelectric characterization, the average crystal domain size increased from 15 to 26 nm. No change in composition was obtained with the annealing treatment. The final residual carbon content within the annealed materials was estimated to be 0.5–1% on the basis of elemental analysis.

Figure 4 shows the electrical conductivity (σ), Seebeck coefficient (S), thermal conductivity (κ), and calculated figure

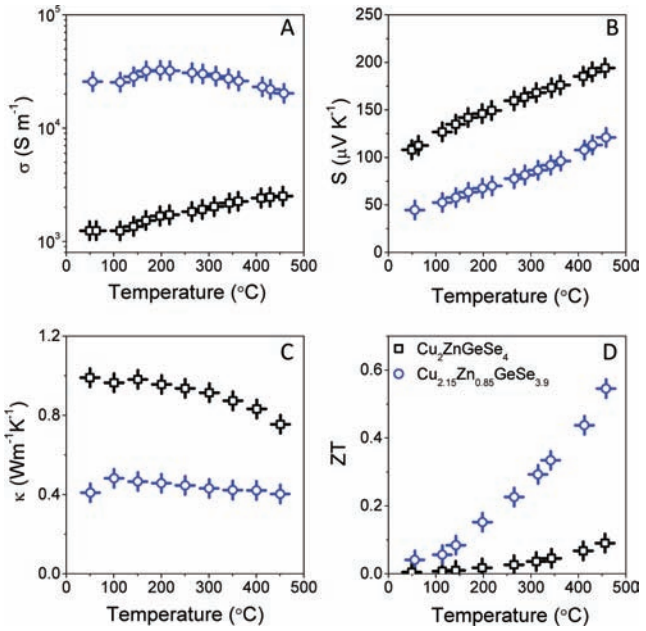

Figure 4. (A) Electrical conductivity, (B) Seebeck coefficient, (C) thermal conductivity, and (D) and figure of merit of CZGS nanomaterials with the following compositions: $Cu_2ZnGeSe_4$ (black □), $Cu_{2.15}Zn_{0.85}GeSe_{3.9}$ (blue ○).

of merit (ZT) of $Cu_2ZnGeSe_4$ and $Cu_{2.15}Zn_{0.85}GeSe_{3.9}$. Thermal conductivity data were obtained from flash diffusivity measurements using the material's mass density and the Dulong–Petit approximation for its specific heat capacity (C_p = 0.34 J g^{-1} K^{-1}). The thermal conductivity was calculated as $\kappa = DC_pd$, where D is the thermal diffusivity, C_p is the heat capacity, and d is the density.

The relatively high electrical conductivities obtained suggest the complete removal of surfactants. The electrical conductivity increased with the partial replacement of Zn by Cu ions, as expected for their different valences. In this regard, it should be highlighted how the compositional control in these quaternary semiconductors offers an accessible method for tuning their carrier concentration. This intrinsic doping strategy is especially appealing in the bottom-up processing of nanomaterials, where the introduction of extrinsic dopants is not an easy task.

As expected for a heavily doped semiconductor, the Seebeck coefficient followed an opposite trend than the electrical conductivity. Lower Seebeck coefficients were obtained for the materials with partial substitution of Zn ions by Cu ions, as this should increase the concentration of holes in the valence band. Finally, the sample with partial substitution of Zn by Cu showed lower thermal conductivity. This lower thermal conductivity is in part associated with the higher degree of disorder introduced in the structure upon replacement of Zn by Cu. However, fine microstructural differences between the two

dx.doi.org/10.1021/ja211952z | J. Am. Chem. Soc. 2012, 134, 4060–4063

nanomaterials having different compositions may also play a significant role.

The final *ZT* values obtained were higher for $Cu_{2.15}Zn_{0.85}GeSe_{3.9}$ than $Cu_2ZnGeSe_4$ because of the improved electrical conductivities and reduced thermal conductivities of the former. The best *ZT* value obtained from this very preliminary composition screening was 0.55 at 450 °C.

In summary, we have detailed a synthetic procedure for producing CZGS nanocrystals with narrow size distribution and controlled compositions. Furthermore, the thermoelectric properties of the nanomaterials obtained after carefully washing the nanocrystals and hot-pressing them into pellets were characterized. By partial replacement of Zn ions by Cu ions, the material's electrical conductivity could be substantially increased, and *ZT* values of up to 0.55 were demonstrated. Further optimization of the material parameters and processing methods could result in materials with higher *ZT* values. While the CZGS nanocrystals presented here show promising thermoelectric properties, we also envisage their potential use as absorber materials in solution-processed solar cells and in other applications, such as topological insulators.

■ ASSOCIATED CONTENT

Supporting Information

Details of the synthesis procedure and characterization techniques and additional compositional maps and HRTEM and TEM images. This material is available free of charge via the Internet at http://pubs.acs.org.

■ AUTHOR INFORMATION

Corresponding Author

acabot@irec.cat

Notes

The authors declare no competing financial interest.

■ ACKNOWLEDGMENTS

This work was supported by the Spanish MICINN Projects MAT2008-05779, MAT2008-03400-E/MAT, MAT2010-15138, ENE2008-03277-E/CON, CSD2009-00050, and CSD2009-00013. M.I. thanks the Spanish MICINN for her Ph.D. Grant. J.A. and R.Z. also acknowledge Generalitat de Catalunya 2009-SGR-770 and XaRMAE. A.C. is thankful for financial support through the Ramon y Cajal Program of the Spanish MICINN.

■ REFERENCES

(1) Guo, Q.; Ford, G. M.; Yang, W.-C.; Walker, B. C.; Stach, E. A.; Hillhouse, H. W.; Agrawal, R. *J. Am. Chem. Soc.* **2010**, *132*, 17384.

(2) Mitzi, D. B.; Gunawan, O.; Todorov, T. K.; Wang, K.; Guha, S. *Sol. Energ. Mat. Sol. C.* **2011**, *95*, 1421.

(3) Samanta, L. K.; Bhar, G. C. *Phys. Status Solidi A* **1977**, *41*, 331.

(4) Liu, M.-L.; Chen, I.-W.; Huang, F.-Q.; Chen, L.-D. *Adv. Mater.* **2009**, *21*, 3808.

(5) (a) Ibáñez, M.; Cadavid, D.; Zamani, R.; García-Castelló, N.; Izquierdo-Roca, V.; Li, W.; Fairbrother, A.; Prades, J. D.; Shavel, A.; Arbiol, J.; Pérez-Rodríguez, A.; Morante, J. R.; Cabot, A. *Chem. Mater.* **2012**, *24*, 562. (b) Fan, F. J.; Yu, B.; Wang, Y. X.; Zhu, Y. L.; Liu, X. J.; Yu, S. H.; Ren, Z. *J. Am. Chem. Soc.* **2011**, *133*, 15910.

(6) Wang, Y. J.; Lin, H.; Das, T.; Hasan, M. Z.; Bansil, A. *New J. Phys.* **2011**, *13*, 085017.

(7) Chen, S.; Gong, X. G.; Duan, C.-G.; Zhu, Z.-Q.; Chu, J.-H.; Walsh, A.; Yao, Y.-G.; Ma, J.; Wei, S.-H. *Phys. Rev. B* **2011**, *83*, 245202.

(8) (a) Shavel, A.; Arbiol, J.; Cabot, A. *J. Am. Chem. Soc.* **2010**, *132*, 4514. (b) Shavel, A.; Cadavid, D.; Ibáñez, M.; Carrete, A.; Cabot, A. *J. Am. Chem. Soc.* **2012**, *134*, 1438.

(9) Davydyuk, G. Ye.; Parasyuk, O. V.; Romanyuk, Ya. E.; Semenyuk, S. A.; Zaremba, V. I.; Piskach, L. V.; Koziol, J. J.; Halka, V. O. *J. Alloys Compd.* **2002**, *339*, 40.

(10) Snyder, G. J.; Toberer, E. S. *Nat. Mater.* **2008**, *7*, 105.

(11) Vineis, C. J.; Shakouri, A.; Majumdar, A.; Kanatzidis, M. G. *Adv. Mater.* **2010**, *22*, 3970.

(12) Schleich, D. M.; Wold, A. *Mater. Res. Bull.* **1997**, *12*, 111.

(13) Lee, C.; Kim, C.-D. *J. Korean Phys. Soc.* **2000**, *37*, 364.

(14) Matsushita, H.; Ichikawa, T.; Katsui, A. *J. Mater. Sci.* **2005**, *40*, 2003.

(15) Chen, S.; Gong, X. G.; Walsh, A.; Wei, S.-H. *Phys. Rev. B* **2009**, *79*, 165211.

(16) Walsh, A.; Chen, S.; Gong, X. G.; Wei, S.-H. *Sol. Cells* **2010**, *4*, 4.

(17) Matsushita, H.; Ochiai, T.; Katsui, A. *J. Cryst. Growth* **2005**, *275*, e995.

(18) Nakamura, S.; Maeda, T.; Wada, T. *Jpn. J. Appl. Phys.* **2010**, *49*, No. 121203.

(19) Romanyuk, Ya. E.; Parasyuk, O. V. *J. Alloys Compd.* **2003**, *348*, 195.

(20) Parasyuk, O. V.; Gulay, L. D.; Romanyuk, Ya. E.; Piskach, L. V. *J. Alloys Compd.* **2001**, *329*, 202.

(21) Doverspike, K.; Dwight, K.; Wold, A. *Chem. Mater.* **1990**, *2*, 194.